

Static Solutions for Plane Strain Problem of Coupled Diffusion and Deformation

Lingjun Yu^a, Xingquan Wang^{b,*}, Lulu Chen^c,
Dongdong Yu^a, Zhaokai Li^a, and Xudong Tang^a

^aBeijing Institute of Mechanical Equipment, Beijing, 100854 China

^bState Key Laboratory of Nonlinear Mechanics, Institute of Mechanics,
Chinese Academy of Sciences, Beijing, 100190 China

^cBeijing Glodwind New Energy Trade Co., Ltd, Beijing, 100176 China

*e-mail: wang_xqhey@yeah.net

Received August 30, 2022; revised November 11, 2022; accepted November 17, 2022

Abstract—The diffusion and deformation coupled problem are considered in many material and engineering areas, and it has been studied on both theory and solution methods. However, the analytical solutions for this problem are relatively fewer, especially for two-dimensional problems. In this paper, based on a diffusion and mechanical coupled continuum model, the plane strain problem in the polar coordinates considering mass diffusion was studied. The relationship between volume strain and mass concentration was deduced by using a displacement potential function, and the analytical expression for concentration was then deduced. To comply with the mechanical boundary conditions, the Airy stress function was applied. The analytical expressions for stress components were also completely determined. After that, a numerical example of a cylinder with variant concentration distribution on its cylindrical surface was given, the results showed that concentration gradient distribution would cause the generation of stresses and the value of stresses positive correlated to the concentration gradient.

Keywords: diffusion-induced stress, analytical solution, Airy stress function, chemo-mechanical coupling

DOI: 10.3103/S0025654423600824

1. INTRODUCTION

When the diffusion equation with mechanical effect term incorporated and the motion equations contain the effect of concentration, this kind of problem is called coupled diffusion and deformation problem. This problem may arise in many materials and engineering areas, including soft materials [1], batteries [2], and biomedicine [3].

The diffusion induced stress was first researched by analogy with the thermal stress by Prussin [4]. Following his work, quantities of theoretical models concerning diffusion and deformation were proposed. These models can be classified into two categories, i.e., the linear and non-linear theories. For nonlinear theories, the large deformation [5], concentration dependent material parameters [6], reaction [7] and plastic flow [8, 9] were considered. Larch and Cahn [10] developed a linear theory of thermochemical equilibrium of solid based on thermodynamics. The linearization method has been employed in many continuum models that diffusion and deformation were coupled [11–14].

Based on these developed models, the concentration and stress distribution of various structures, like, nanowire [15], composite structures [16, 17], thin film [18, 19] were studied. Mostly, the numerical simulation or numerical methods were used, analytical solutions usually appear in one-dimensional cases [20–22].

In this paper, based on a diffusion and deformation coupled linear model, a plane strain problem in the polar coordinates considering steady state mass diffusion was analytically solved by using a displacement potential function and Airy stress function. Then a traction free cylinder long enough with half of its flank under constant concentration boundary conditions were analysed. The numerical results showed that the gradient distribution of concentration would cause the generation of stresses because of the defor-

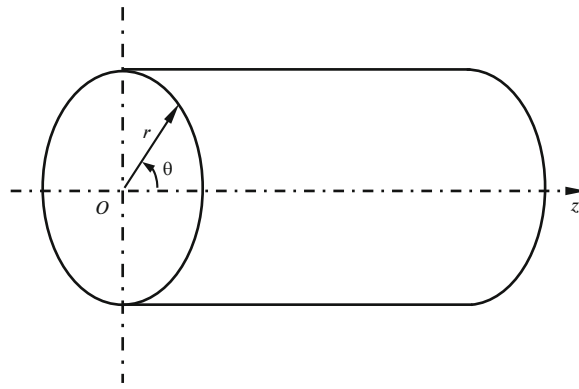


Fig. 1. The sketch of a circular cylinder.

mation mismatch induced by the difference of concentration. The value of stresses would increase with concentration gradient.

2. BASIC FORMULATIONS OF COUPLED DIFFUSION AND DEFORMATION

Following the linear continuum model [14], a homogenous isotropic active media with steady mass flow, the concentration will satisfy the equation

$$Ag\Delta c + Ab\Delta e = 0, \tag{2.1}$$

where A is the species mobility, g is the scalar chemistry modulus, $e = \text{div } \mathbf{u}$ represents the volume strain, and coefficient b is chemistry-strain modulus that can be expressed by Lamé constants λ , G and chemical dilation coefficient β as

$$b = -(3\lambda + 2G)\beta. \tag{2.2}$$

The inertia term and body force are ignored, the basic equation of motion is

$$G\Delta \mathbf{u} + (\lambda + G)\nabla(\nabla \cdot \mathbf{u}) + b\nabla c = 0. \tag{2.3}$$

3. GENERAL SOLUTION FOR A LONG CYLINDER

Considering a circular cylinder with radius a as showed in Fig. 1, and supposed that the applied tractions on the cylindrical boundaries which parallel to the z -axis and the species concentration distribution are independent of the axial coordinate z .

It is convenient to suppose that the diffusion only occurred in the radial direction and the cylinder is long enough, so that the problem can be simplified as plane strain problem. The polar coordinates are adopted here and the Laplace operator in polar coordinates is $\Delta = \frac{\partial^2}{\partial r^2} + \frac{1}{r} \frac{\partial}{\partial r} + \frac{1}{r^2} \frac{\partial^2}{\partial \theta^2}$. To analyze this chemo-mechanical coupled problem, the displacement method is used, and a chemical displacement potential function ψ is introduced. Equation (2.3) in polar coordinates can be stated as

$$(1 - 2\nu)\Delta u_r + \frac{\partial e}{\partial r} = -\frac{b}{\lambda + G} \frac{\partial c}{\partial r}, \tag{3.1}$$

$$(1 - 2\nu)\Delta u_\theta + \frac{1}{r} \frac{\partial e}{\partial \theta} = -\frac{b}{\lambda + G} \frac{1}{r} \frac{\partial c}{\partial \theta}, \tag{3.2}$$

where $e = \frac{\partial u_r}{\partial r} + \frac{u_r}{r} + \frac{\partial u_\theta}{r \partial \theta}$ is the volume strain, u_r and u_θ represent radial displacement and circumferential displacement respectively. The particular solution of Eqs. (3.1) and (3.2) can be related to the chemical displacement potential function ψ as follows

$$u_r = \frac{\partial \psi}{\partial r} \quad u_\theta = \frac{1}{r} \frac{\partial \psi}{\partial \theta}. \tag{3.3}$$

From Eq. (3.3), it is obviously to have $e = \Delta\psi$, then Eqs. (3.1) and (3.2) are written as

$$(1 - \nu) \frac{\partial}{\partial r} (\Delta\psi) = -\frac{b}{\lambda + G} \frac{\partial c}{\partial r}. \quad (3.4)$$

$$(1 - \nu) \frac{1}{r} \frac{\partial}{\partial \theta} (\Delta\psi) = -\frac{b}{\lambda + G} \frac{1}{r} \frac{\partial c}{\partial \theta}. \quad (3.5)$$

And these two partial differential equations can be satisfied when the chemical displacement potential ψ is the solution of following equation

$$\Delta\psi = \frac{1 + \nu}{1 - \nu} \beta c. \quad (3.6)$$

The stresses expressions corresponding to the chemical displacement potential ψ are

$$\sigma_{rr} = -\frac{E}{1 + \nu} \left(\frac{1}{r} \frac{\partial \psi}{\partial r} + \frac{1}{r^2} \frac{\partial^2 \psi}{\partial \theta^2} \right), \quad (3.7)$$

$$\sigma_{\theta\theta} = -\frac{E}{1 + \nu} \frac{\partial^2 \psi}{\partial r^2}, \quad (3.8)$$

$$\sigma_{r\theta} = \frac{E}{1 + \nu} \frac{\partial}{\partial r} \left(\frac{1}{r} \frac{\partial \psi}{\partial \theta} \right) \quad (3.9)$$

and the stress component in z direction is

$$\sigma_{zz} = \nu (\sigma_{rr} + \sigma_{\theta\theta}) - E\beta c. \quad (3.10)$$

From Eq. (3.6) and accommodate the relations between volume strain e and potential function ψ , the diffusion equation can be written as

$$A \left(g - \frac{b^2}{\lambda + G} \right) \Delta c = 0. \quad (3.11)$$

We note that $M = A \left(g - \frac{b^2}{\lambda + G} \right)$, and the chemical boundary condition about concentration is given as follows

$$c(a, \theta) = G(\theta). \quad (3.12)$$

It should be mentioned that the conventional enforced chemical boundary condition is the specification of the chemical potential which is usually used for water absorption or dehydration [1, 23]. However, the chemical boundary condition about concentration is also frequently used in the analysis of batteries or solute transportation [24, 25], where the diffusion induced stresses are more concerned about. Here, we are focused on the analytical solution of plane strain problem about mass diffusion induced stresses, this may throw light on the stress analysis during battery charging and discharging process, so the boundary condition about concentration is used.

The solution of steady-state equation (3.11) with boundary condition (3.12) can be easily obtained as

$$c(r, \theta) = a_0 + \sum_{m=1}^{\infty} \left(\frac{r}{a} \right)^m [a_m \cos(m\theta) + b_m \sin(m\theta)] \quad (3.13)$$

and the coefficients are

$$\begin{aligned} a_0 &= \frac{1}{2\pi} \int_0^{2\pi} G(\theta) d\theta, \\ a_m &= \frac{1}{\pi} \int_0^{2\pi} G(\theta) \cos(m\theta) d\theta, \\ b_m &= \frac{1}{\pi} \int_0^{2\pi} G(\theta) \sin(m\theta) d\theta. \end{aligned} \quad (3.14)$$

Using Eq. (3.13) in Eq. (3.6), the chemical displacement potential is obtained as

$$\psi = -\frac{(1 + a^2 - r^2)\beta(a^2 - r^2)}{(1 - \nu)4} \left(a_0 + \sum_{m=1}^{\infty} \frac{1}{n+1} \left(\frac{r}{a}\right)^m [a_m \cos(m\theta) + b_m \sin(m\theta)] \right). \tag{3.15}$$

Then the stresses in (3.7)–(3.9) are expressed as

$$\sigma'_{rr} = -\frac{E\beta}{1 - \nu} \left\{ \begin{aligned} &\frac{1}{2}a_0 + \frac{1}{4} \sum_{m=1}^{\infty} \frac{m(m-1)}{m+1} \left(\frac{r}{a}\right)^{m-2} [a_m \cos(m\theta) + b_m \sin(m\theta)] \\ &-\frac{1}{4} \sum_{m=1}^{\infty} (m-2) \left(\frac{r}{a}\right)^m [a_m \cos(m\theta) + b_m \sin(m\theta)] \end{aligned} \right\}, \tag{3.16}$$

$$\sigma'_{\theta\theta} = -\frac{E\beta}{1 - \nu} \left\{ \begin{aligned} &\frac{1}{2}a_0 - \frac{1}{4} \sum_{m=1}^{\infty} \frac{m(m-1)}{m+1} \left(\frac{r}{a}\right)^{m-2} [a_m \cos(m\theta) + b_m \sin(m\theta)] \\ &+\frac{1}{4} \sum_{m=1}^{\infty} (m+2) \left(\frac{r}{a}\right)^m [a_m \cos(m\theta) + b_m \sin(m\theta)] \end{aligned} \right\}, \tag{3.17}$$

$$\sigma'_{r\theta} = \frac{E\beta}{1 - \nu} \left\{ \begin{aligned} &-\frac{1}{4} \sum_{m=1}^{\infty} \frac{m(m-1)}{m+1} \left(\frac{r}{a}\right)^{m-2} [b_m \cos(m\theta) - a_m \sin(m\theta)] \\ &+\frac{1}{4} \sum_{m=1}^{\infty} m \left(\frac{r}{a}\right)^m [b_m \cos(m\theta) - a_m \sin(m\theta)] \end{aligned} \right\}. \tag{3.18}$$

Granted that the cylindrical surface of the circular cylinder is free of stresses, however a non-zero surface stresses $(\sigma'_{rr}, \sigma'_{r\theta})$ is given by the stresses expressions of (3.16)–(3.18)

$$(\sigma'_{rr})_{r=a} = -\frac{E\beta}{1 - \nu} \left\{ \frac{1}{2}a_0 + \frac{1}{2} \sum_{m=1}^{\infty} \frac{1}{m+1} [a_m \cos(m\theta) + b_m \sin(m\theta)] \right\}, \tag{3.19}$$

$$(\sigma'_{r\theta})_{r=a} = \frac{E\beta}{1 - \nu} \left\{ \frac{1}{2} \sum_{m=1}^{\infty} \frac{m}{m+1} [b_m \cos(m\theta) - a_m \sin(m\theta)] \right\}. \tag{3.20}$$

To comply with the stress boundary condition, the complementary stress should be introduced to cancelling the surface stresses of Eqs. (3.19) and (3.20). Therefore, forces equal to (3.19) and (3.20) but in opposite directions are taken as surface loads to seek the solution of the complementary stress, and the general stress function expressed in polar coordinates is used. Noting that the first term of the stress in brackets of Eq. (3.19) is symmetrical to the origin of coordinates, and the other terms as well as the expression of Eq. (3.20) is the stress proportional to $\sin(m\theta)$ or $\cos(m\theta)$ acting on the outer surface of the cylinder. Accordingly, the Airy stress function can be assumed as

$$\begin{aligned} \phi &= k_0 r^2 + k_1 r^3 \cos \theta + p_1 r^3 \sin \theta \\ &+ \sum_{m=2}^{\infty} (k_m r^{m+2} + l_m r^m) \cos(m\theta) + \sum_{m=2}^{\infty} (p_m r^{m+2} + q_m r^m) \sin(m\theta). \end{aligned} \tag{3.21}$$

The corresponding stress components are

$$\begin{aligned} \sigma_{rr} &= \frac{1}{r} \frac{\partial \phi}{\partial r} + \frac{1}{r^2} \frac{\partial^2 \phi}{\partial \theta^2} = 2k_0 + 2k_1 r \cos \theta + 2p_1 r \sin \theta \\ &- \sum_{m=2}^{\infty} [(m+1)(m-2)k_m r^m + m(m-1)l_m r^{m-2}] \cos(m\theta) \\ &- \sum_{m=2}^{\infty} [(m+1)(m-2)p_m r^m + m(m-1)q_m r^{m-2}] \sin(m\theta), \end{aligned} \tag{3.22}$$

$$\begin{aligned} \sigma_{\theta\theta} &= \frac{\partial^2 \phi}{\partial r^2} = 2k_0 + 6k_1 r \cos \theta + 6p_1 r \sin \theta \\ &+ \sum_{m=2}^{\infty} \left[(m+1)(m+2)k_m r^m + m(m-1)l_m r^{m-2} \right] \cos(m\theta) \\ &+ \sum_{m=2}^{\infty} \left[(m+1)(m+2)p_m r^m + m(m-1)q_m r^{m-2} \right] \sin(m\theta), \end{aligned} \quad (3.23)$$

$$\begin{aligned} \sigma_{r\theta} &= -\frac{\partial}{\partial r} \left(\frac{1}{r} \frac{\partial \phi}{\partial \theta} \right) = -2p_1 r \cos \theta + 2k_1 r \sin \theta \\ &- \sum_{m=2}^{\infty} \left[m(m+1)p_m r^m + (m-1)q_m r^{m-2} \right] \cos(m\theta) \\ &+ \sum_{m=2}^{\infty} \left[m(m+1)k_m r^m + (m-1)l_m r^{m-2} \right] \sin(m\theta). \end{aligned} \quad (3.24)$$

At the cylinder surface, they come to

$$\begin{aligned} (\sigma_{rr})_{r=a} &= 2k_0 + 2k_1 a \cos \theta + 2p_1 a \sin \theta \\ &- \sum_{m=2}^{\infty} \left[(m+1)(m-2)k_m a^m + m(m-1)l_m a^{m-2} \right] \cos(m\theta) \\ &- \sum_{m=2}^{\infty} \left[(m+1)(m-2)p_m a^m + m(m-1)q_m a^{m-2} \right] \sin(m\theta), \end{aligned} \quad (3.25)$$

$$\begin{aligned} (\sigma_{r\theta})_{r=a} &= -2p_1 a \cos \theta + 2k_1 a \sin \theta \\ &- \sum_{m=2}^{\infty} \left[m(m+1)p_m a^m + (m-1)q_m a^{m-2} \right] \cos(m\theta) \\ &+ \sum_{m=2}^{\infty} \left[m(m+1)k_m a^m + (m-1)l_m a^{m-2} \right] \sin(m\theta). \end{aligned} \quad (3.26)$$

The stresses expressions of (3.25) and (3.26) should be equal but reverse to the stresses of (3.19) and (3.20) respectively. Comparing each term of these expressions after sorting, the coefficients in Eq. (3.21) are obtained as

$$\begin{aligned} k_0 &= \frac{E\beta a_0}{4(1-\nu)} & k_1 &= \frac{E\beta a_1}{8(1-\nu)a} & p_1 &= \frac{E\beta b_1}{8(1-\nu)a}, \\ k_m &= \frac{E\beta}{1-\nu} \left[\frac{(m^2+1)}{2a^m(m+1)^2(m^2-m+2)} a_m \right], \\ l_m &= -\frac{E\beta}{1-\nu} \left[\frac{m}{2a^{m-2}(m+1)(m^2-m+2)} a_m \right], \\ p_m &= \frac{E\beta}{1-\nu} \left[\frac{(m^2+1)}{2a^m(m+1)^2(m^2-m+2)} b_m \right], \\ q_m &= -\frac{E\beta}{1-\nu} \left[\frac{m}{2a^{m-2}(m+1)(m^2-m+2)} b_m \right]. \end{aligned} \quad (3.27)$$

Using the coefficients of Eq. (3.27) in the stresses expressions (3.22)–(3.24), the complementary stresses are obtained as following

$$\sigma_{rr} = \frac{E\beta}{1-\nu} \left\{ \begin{aligned} & \frac{1}{2}a_0 + \frac{a_1r}{4a} \cos \theta + \frac{b_1r}{4a} \sin \theta \\ & - \sum_{m=2}^{\infty} \left[\frac{(m^2+1)(m-2)a_m}{2(m+1)(m^2-m+2)} \left(\frac{r}{a}\right)^m \right] \cos(m\theta) \\ & + \sum_{m=2}^{\infty} \left[\frac{m^2(m-1)a_m}{2(m+1)(m^2-m+2)} \left(\frac{r}{a}\right)^{m-2} \right] \cos(m\theta) \\ & - \sum_{m=2}^{\infty} \left[\frac{(m^2+1)(m-2)b_m}{2(m+1)(m^2-m+2)} \left(\frac{r}{a}\right)^m \right] \sin(m\theta) \\ & + \sum_{m=2}^{\infty} \left[\frac{m^2(m-1)b_m}{2(m+1)(m^2-m+2)} \left(\frac{r}{a}\right)^{m-2} \right] \sin(m\theta) \end{aligned} \right\}, \tag{3.28}$$

$$\sigma_{\theta\theta} = \frac{E\beta}{1-\nu} \left\{ \begin{aligned} & \frac{1}{2}a_0 + \frac{3a_1r}{4a} \cos \theta + \frac{3b_1r}{4a} \sin \theta \\ & + \sum_{m=2}^{\infty} \left[\frac{(m+2)(m^2+1)a_m}{2(m+1)(m^2-m+2)} \left(\frac{r}{a}\right)^m \right] \cos(m\theta) \\ & - \sum_{m=2}^{\infty} \left[\frac{m^2(m-1)a_m}{2(m+1)(m^2-m+2)} \left(\frac{r}{a}\right)^{m-2} \right] \cos(m\theta) \\ & + \sum_{m=2}^{\infty} \left[\frac{(m+2)(m^2+1)b_m}{2(m+1)(m^2-m+2)} \left(\frac{r}{a}\right)^m \right] \sin(m\theta) \\ & - \sum_{m=2}^{\infty} \left[\frac{m^2(m-1)b_m}{2(m+1)(m^2-m+2)} \left(\frac{r}{a}\right)^{m-2} \right] \sin(m\theta) \end{aligned} \right\}, \tag{3.29}$$

$$\sigma_{r\theta} = \frac{E\beta}{1-\nu} \left\{ \begin{aligned} & -\frac{b_1r}{4a} \cos \theta + \frac{a_1r}{4a} \sin \theta \\ & - \sum_{m=2}^{\infty} \left[\frac{b_m m(m^2+1)}{2(m+1)(m^2-m+2)} \left(\frac{r}{a}\right)^m \right] \cos(m\theta) \\ & + \sum_{m=2}^{\infty} \left[\frac{b_m m(m-1)}{2(m+1)(m^2-m+2)} \left(\frac{r}{a}\right)^{m-2} \right] \cos(m\theta) \\ & + \sum_{m=2}^{\infty} \left[\frac{a_m m(m^2+1)}{2(m+1)(m^2-m+2)} \left(\frac{r}{a}\right)^m \right] \sin(m\theta) \\ & - \sum_{m=2}^{\infty} \left[\frac{a_m m(m-1)}{2(m+1)(m^2-m+2)} \left(\frac{r}{a}\right)^{m-2} \right] \sin(m\theta) \end{aligned} \right\}. \tag{3.30}$$

The actual in-plane stress components are now completely determined as the sum of particular solution expressions (3.16)–(3.18) and the complementary stress (3.28)–(3.30) respectively. Then the axial stress component can be found by Eq. (3.10).

4. APPLICATION

Assuming that the radius of the cylinder is $a = 1$, the concentration on the upper half of its circumference is kept at $c_0 = 2.3 \times 10^4$ mol/m³ and concentration on the lower half is kept at zero, and no traction on the circumference surface. The material parameters are set as $\nu = 0.3$, $E = 1.9 \times 10^{11}$ Pa, $\beta = 1.167 \times 10^{-6}$ m³/mol. Then the concentration boundary conditions are described by

$$c(1, \theta) = G(\theta) = \begin{cases} c_0 & \text{if } 0 < \theta < \pi, \\ 0 & \text{if } \pi < \theta < 2\pi. \end{cases} \quad (4.1)$$

Substituted $G(\theta)$ into Eq. (3.14), the coefficients are determined

$$a_0 = \frac{1}{2\pi} \int_0^\pi c_0 d\theta = \frac{c_0}{2}, \quad (4.2)$$

$$a_m = \frac{1}{\pi} \int_0^\pi c_0 \cos(m\theta) d\theta = 0, \quad (4.3)$$

$$b_m = \frac{1}{\pi} \int_0^\pi c_0 \sin(m\theta) d\theta = \frac{c_0}{m\pi} [1 - \cos(m\pi)]. \quad (4.4)$$

Then,

$$c(r, \theta) = \frac{c_0}{2} + \frac{c_0}{\pi} \sum_{m=1}^{\infty} \frac{1}{m} [1 - \cos(m\pi)] \left(\frac{r}{a}\right)^m \sin(m\theta) \quad (4.5)$$

The complete stress expressions are as follows

$$\sigma_{rr} = \frac{E\beta}{1-\nu} \left\{ \frac{c_0}{\pi} \sum_{m=2}^{\infty} \frac{(m-2)(m-1)^2}{4(m+1)(m^2-m+2)} \left[\left(\frac{r}{a}\right)^m - \left(\frac{r}{a}\right)^{m-2} \right] [1 - \cos(m\pi)] \sin(m\theta) \right\}, \quad (4.6)$$

$$\sigma_{\theta\theta} = \frac{E\beta}{1-\nu} \left\{ \frac{c_0}{\pi} \sum_{m=2}^{\infty} \left[\frac{(m+2)(m-1)^2}{4(m+1)(m^2-m+2)} \left(\frac{r}{a}\right)^m - \frac{(m-2)(m-1)^2}{4(m+1)(m^2-m+2)} \left(\frac{r}{a}\right)^{m-2} \right] [1 - \cos(m\pi)] \sin(m\theta) \right\}, \quad (4.7)$$

$$\sigma_{r\theta} = \frac{E\beta}{1-\nu} \left\{ \frac{c_0}{\pi} \sum_{m=2}^{\infty} \frac{m(m-1)^2}{4(m+1)(m^2-m+2)} \left[\left(\frac{r}{a}\right)^m - \left(\frac{r}{a}\right)^{m-2} \right] [1 - \cos(m\pi)] \cos(m\theta) \right\}, \quad (4.8)$$

$$\begin{aligned} \sigma_{zz} = & -\frac{E\beta c_0}{2} - \frac{E\beta}{1-\nu} \frac{c_0}{\pi} \sum_{m=1}^{\infty} \frac{1}{m} \left(\frac{r}{a}\right)^m [1 - \cos(m\pi)] \sin(m\theta) \\ & + \frac{\nu E\beta}{1-\nu} \frac{c_0}{\pi} \sum_{m=1}^{\infty} \frac{1}{m} \frac{2(m^2+1)}{m(m+1)(m^2-m+2)} \left(\frac{r}{a}\right)^m [1 - \cos(m\pi)] \sin(m\theta). \end{aligned} \quad (4.9)$$

5. RESULTS AND DISCUSSION

Based on the obtained analytical expressions, the distributions of concentration and stresses on the cross section of the cylinder were obtained. Figure 2 showed the distribution of concentration on the cross section of the cylinder. The boundary conditions of concentration were satisfied and the concentration in the cylinder was distributed gradually from upper half to lower half. The concentration gradients near the outer circumference at the angles of 0 and 180 degrees were larger. The concentration was also bilateral symmetrically distributed, and the concentration at the centre of the cross section was the average of the concentration on the boundary.

The radial stress distribution of the cylinder on cross section was showed in Fig. 3. The radial stress at the outer circumference was zero for the outer surface of the cylinder is traction free. Unlike the axisymmetric cases where the radial stress in the cylinder went to zero at the steady state, the radial stress still existed in this case because of the deformation mismatch induced by the difference of concentration. The radial stress appeared to be larger at the points where the gradient of concentration was larger. And the radial stress was antisymmetric distributed on the upper and lower half of the cross section. That is, the radial stress in the upper and lower half was equal in magnitude but opposite in direction.

Figure 4 showed the distribution of hoop stress on the cross section. It was also antisymmetric distributed, and the values of the hoop stress on the regions which near the angles of 0 and 180 degrees at the outer circumference of the cross section were larger, but tensile on the region in upper half, compressive on the region in lower half. This stress distribution was to meet the needs of circumferential deformation compatibility. For the upper half region of the cross section, the circumferential deformation was

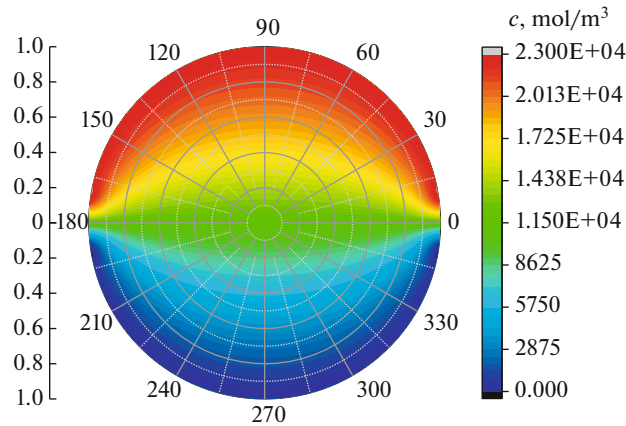


Fig. 2. The distribution of concentration on the cross section.

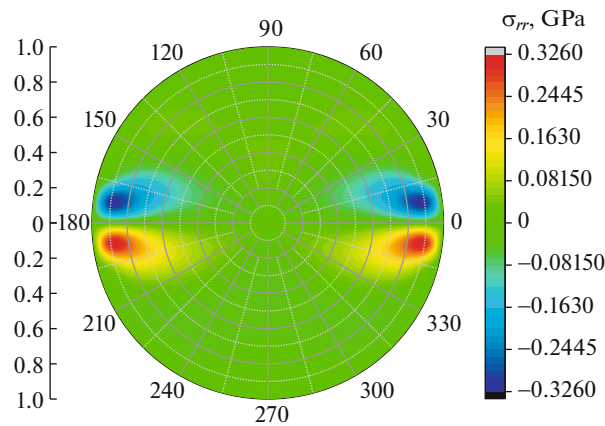


Fig. 3. Radial stress distribution on the cross section.

restricted where the concentration was large and the circumferential deformation was promoted where concentration is small, so the hoop stress is tensile on the regions near the angles of 0 and 180 degrees at the outer circumference. While for the lower half region of the cross section, the stress distribution was opposite to that of upper half was for the same reason.

The distribution of shear stress on the cross section of cylinder was showed in Fig. 5. The shear stress was zero at the boundary of the cross section to meet the boundary conditions. And it was antisymmetric distributed about the vertical axis of the cross section, because the directions of shear stress in the two sides of the vertical axis were opposite. For the left half region of the cross section, the shear stress is positive near the angle of 180 degree along the radius, while negative on other parts of the region. The increase of concentration would cause the expansion of volume, however, the concentration in consideration was gradiently distributed, the cross section would change from circular to elliptical, resulted in the generation of shear stress.

From Fig. 6, we noted that the axial stress in the cross section was compressive and it was also gradiently distributed. The value of the compressive axial stress was positively correlated with the concentration. It was because the deformation in axial direction was confined, the diffusion induced axial expansion deformation were neutralized by the deformation caused by compressive axial stress.

6. CONCLUSIONS

In this work, based on a diffusion and mechanical coupled continuum model, a plane strain problem in the polar coordinates considering steady state mass diffusion was analysed. The analytical expressions for concentration and stresses were obtained by using a displacement potential function and the Airy stress

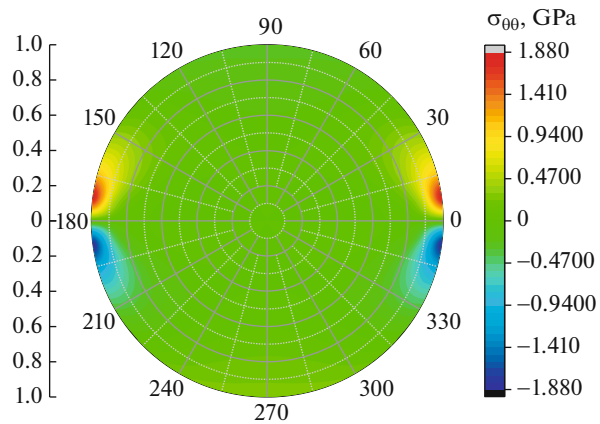


Fig. 4. Hoop stress distribution on the cross section.

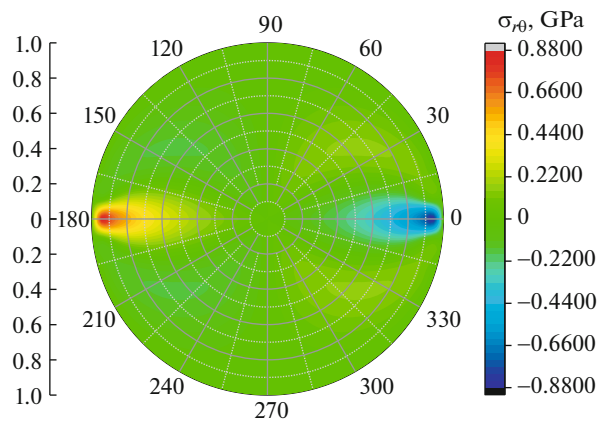


Fig. 5. Shear stress distribution on the cross section.

function. A numerical example of a traction free cylinder with half of its flank under constant concentration was given, its steady state stresses and concentration distributions on the cross section were obtained. The results showed that the gradiently distributed concentration would lead to the generation of stress and the value of stress increased with the gradient of concentration.

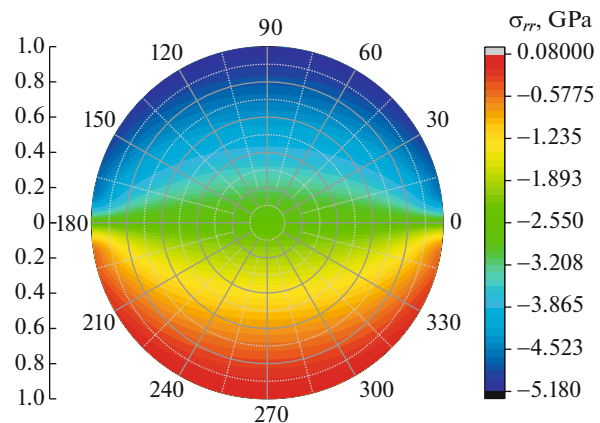


Fig. 6. Axial stress distribution on the cross section.

REFERENCES

1. S. Xu and Z. Liu, "Coupled theory for transient responses of conductive hydrogels with multi-stimuli," *J. Mech. Phys. Solids* **143**, 104055 (2020).
<https://doi.org/10.1016/j.jmps.2020.104055>
2. S. Zhang, "Chemomechanical modeling of lithiation-induced failure in high-volume-change electrode materials for lithium ion batteries," *Npj Computat. Mater.* **3**, 7 (2017).
<https://doi.org/10.1038/s41524-017-0009-z>
3. A. T. Vuong, A.D. Rauch, and W. A. Wall, "A biochemo-mechano coupled, computational model combining membrane transport and pericellular proteolysis in tissue mechanics," *Proc. Roy. Soc. A – Math. Phys. Eng. Sci.* **473** (2199) (2017).
<https://doi.org/10.1098/rspa.2016.0812>
4. S. Prussin, "Generation and distribution of dislocations by solute diffusion," *J. Appl. Phys.* **32**, 1876–1881 (1961).
<https://doi.org/10.1063/1.1728256>
5. L. Anand, "A Cahn-Hilliard-type theory for species diffusion coupled with large elastic-plastic deformations," *J. Mech. Phys. Solids* **60**, 1983–2002 (2012).
<https://doi.org/10.1016/j.jmps.2012.08.001>
6. C. Zheng, T. Wu, and Z. Deng, "Torsion of hydrogel cylinder with a chemo-mechanical coupled nonlinear elastic theory," *Int. J. Solids Struct.* **248**, 111670 (2022).
<https://doi.org/10.1016/j.ijsolstr.2022.111670>
7. A. Afshar and C. V. Di Leo, "A thermodynamically consistent gradient theory for diffusion–reaction–deformation in solids: Application to conversion-type electrodes," *J. Mech. Phys. Solids* **151**, 104368 (2021).
<https://doi.org/10.1016/j.jmps.2021.104368>
8. B. Qin and Z. Zhong, "A diffusion–reaction–deformation coupling model for lithiation of silicon electrodes considering plastic flow at large deformation," *Arch. Appl. Mech.* **91**, 2713–2733 (2021).
<https://doi.org/10.1007/s00419-021-01919-z>
9. A. F. Bower, P. R. Guduru, and V.A. Sethuraman, "A finite strain model of stress, diffusion, plastic flow, and electrochemical reactions in a lithium-ion half-cell," *J. Mech. Phys. Solids* **59**, 804–828 (2011).
<https://doi.org/10.1016/j.jmps.2011.01.003>
10. F. Larché and J.W. Cahn, "A linear theory of thermochemical equilibrium of solids under stress," *Acta Met.* **21**, 1051–1063 (1973).
[https://doi.org/10.1016/0001-6160\(73\)90021-7](https://doi.org/10.1016/0001-6160(73)90021-7)
11. X. Gao, D. Fang and J. Qu, "A chemo-mechanics framework for elastic solids with surface stress," *Proc. Roy. Soc. A - Math. Phys. Eng. Sci.* **471** (2015).
<https://doi.org/10.1098/rspa.2015.0366>
12. X. L. Zhang and Z. Zhong, "A coupled theory for chemically active and deformable solids with mass diffusion and heat conduction," *J. Mech. Phys. Solids* **107**, 49–75 (2017).
<https://doi.org/10.1016/j.jmps.2017.06.013>
13. X. Wang, X. Liu, and Q. Yang, "Transient analysis of diffusion-induced stress for hollow cylindrical electrode considering the end bending effect," *Acta Mech.* **232**, 3591–3609 (2021).
<https://doi.org/10.1007/s00707-021-03014-4>
14. X.-Q. Wang and Q.-S. Yang, "An analytical solution for chemo-mechanical coupled problem in deformable sphere with mass diffusion," *Int. J. Appl. Mech.* **12** (7), 2050076 (2020).
<https://doi.org/10.1142/s1758825120500763>
15. K. Zhang, Y. Li, F. Wang, et al., "Stress effect on self-limiting lithiation in silicon-nanowire electrode," *Appl. Phys. Expr.* **12**, 045004 (2019).
<https://doi.org/10.7567/1882-0786/ab0ce8>
16. M. Holzapfel, H. Buqa, W. Scheifele, et al., "A new type of nano-sized silicon/carbon composite electrode for reversible lithium insertion," *Chem. Commun., Iss. 12*, 1566–1568 (2005).
<https://doi.org/10.1039/b417492e>
17. J. Wang and W. Cui, "A cross-scale hygro-mechanical coupling model for hollow glass bead/resin composite materials," *Int. J. Solids Struct.* **264**, 112104 (2023).
<https://doi.org/10.1016/j.ijsolstr.2023.112104>
18. M. Liu, "Finite element analysis of lithiation-induced decohesion of a silicon thin film adhesively bonded to a rigid substrate under potentiostatic operation," *Int. J. Solids Struct.* **67–68**, 263–271 (2015).
<https://doi.org/10.1016/j.ijsolstr.2015.04.026>
19. X. Xiao, P. Liu, M. W. Verbrugge, et al., "Improved cycling stability of silicon thin film electrodes through patterning for high energy density lithium batteries," *J. Power Sources* **196**, 1409–1416 (2011).
<https://doi.org/10.1016/j.jpowsour.2010.08.058>

20. X.-Q. Wang and Q.-S. Yang, “A general solution for one dimensional chemo-mechanical coupled hydrogel rod,” *Acta Mech. Sin.* **34**, 392–399 (2017).
<https://doi.org/10.1007/s10409-017-0728-x>
21. Y. Suo and S. Shen, “Analytical solution for one-dimensional coupled non-Fick diffusion and mechanics,” *Arch. Appl. Mech.* **83**, 397–411 (2012).
<https://doi.org/10.1007/s00419-012-0687-4>
22. Y. Song, B. Lu, X. Ji, et al., “Diffusion induced stresses in cylindrical lithium-ion batteries: analytical solutions and design insights,” *J. Electrochem. Soc.* **159**, A2060–A2068 (2012).
<https://doi.org/10.1149/2.079212jes>
23. E. Y. Denisyuk, “Problems of the mechanics of polymer gels with unilateral constraints,” *Mech. Solids* **57**, 292–306 (2022).
<https://doi.org/10.3103/S0025654422020054>
24. Y. Zhao, P. Stein, Y. Bai, et al., “A review on modeling of electro-chemo-mechanics in lithium-ion batteries,” *J. Power Sources* **413**, 259–283 (2019).
<https://doi.org/10.1016/j.jpowsour.2018.12.011>
25. J. Chen, H. Wang, K. M. Liew, et al., “A fully coupled chemomechanical formulation with chemical reaction implemented by finite element method,” *J. Appl. Mech.* **86**, 041006 (2019).
<https://doi.org/10.1115/1.4042431>